Available online at www.sciencedirect.com

SciVerse ScienceDirect

Ceramics International 38 (2012) 3969–3976

CERAMICS INTERNATIONAL

www.elsevier.com/locate/ceramint

Systemic analysis of MgO hydration effects on alumina–magnesia refractory castables

T.M. Souza [a,*], M.A.L. Braulio [a], A.P. Luz [a], P. Bonadia [b], V.C. Pandolfelli [a]

[a] Federal University of São Carlos, Materials Engineering Department, Materials Microstructure Engineering Group (GEMM), FIRE Associate Laboratory, Rod. Washington Luiz, km 235, 13565-905 São Carlos, SP, Brazil

[b] Magnesia Refratários S.A., Research and Development Center, Praça Louis Ensch, 240 Contagem, MG, Brazil

Received 16 January 2012; accepted 20 January 2012
Available online 27 January 2012

Abstract

The use of magnesia sources with high specific surface area and small particle size in the Al_2O_3–MgO system can induce faster in situ spinel ($MgAl_2O_4$) formation in castable compositions, improving the slag corrosion resistance. However, the higher reactivity of these raw materials lead to an intensive brucite formation (followed by volumetric expansion), spoiling the castable's properties during the curing and drying steps. Considering these aspects, a systemic analysis of three magnesia sources (dead-burnt and caustic ones) was carried out in order to evaluate: (1) their hydration impact on the refractory castables properties, and (2) their bonding ability in cement-free compositions. Mechanical strength, thermogravimetric and Young's modulus tests were conducted during the castables' curing and drying steps. According to the results, the elastic modulus measurement is an efficient tool to evaluate the magnesia hydration. The addition of proper amounts of calcium aluminate cement and/or silica fume to the castables can inhibit the crack formation and provide suitable mechanical properties. The results also show that under certain conditions, MgO can be used as a binder, replacing calcium aluminate cement and leading to a significant reduction in the castables costs with no drawbacks to their refractoriness.

© 2012 Elsevier Ltd and Techna Group S.r.l. All rights reserved.

Keywords: MgO; Hydration; Young's modulus; Refractory castables

1. Introduction

The in situ spinel ($MgAl_2O_4$) formation in refractory castables usually takes place at temperatures above 1200 °C and it is affected by various parameters: the aggregate sources, the silica fume content, the MgO grain size and surface area, among others [1–5].

Coarser MgO particles present lower reactivity, whereas magnesia sources with higher specific surface area induce faster spinel formation at lower temperatures [3–5]. Despite this advantage, adding reactive magnesia sources to castable compositions has been avoided, in order to inhibit the hydration drawbacks during the curing and drying steps. MgO hydration is followed by an expressive volumetric expansion due to the density difference between magnesia ($\rho_{MgO} = 3.53$ g cm^{-3}) and brucite ($\rho_{Mg(OH)_2} = 2.40$ g cm^{-3}), resulting in crack formation and refractory properties damage. Therefore, in recent years, some efforts were made for the development of anti-damage and/or anti-hydration techniques [6–9].

As suggested by some authors [8,10,11], calcium aluminate cements (CAC) can lead to higher green mechanical strength levels and, thus, inhibit the damages (cracking) related to the magnesium hydroxide formation [8]. However, considering that calcium hexaluminate (CA_6) generation at high temperatures (>1400 °C) results in further volumetric expansion, an optimized amount of cement should be selected [11]. On the other hand, silica fume can chemically act as an anti-hydration additive, reducing the reaction rate by the precipitation of a magnesium silicate hydrated phase at the MgO particle surface [7,12]. Thus, the addition of silica fume with CAC could be an alternative to control the deleterious effects associated with the brucite formation. Nevertheless, their added contents must be appropriately designed, as low melting temperature phases (i.e., $CaAl_2Si_2O_8$ and $Ca_2Al_2SiO_7$) can be generated in the refractory matrix, affecting the castable thermo-mechanical properties [13].

* Corresponding author. Tel.: +55 16 33518253; fax: +55 16 33615404.
E-mail address: uaitiago@gmail.com (T.M. Souza).

0272-8842/$36.00 © 2012 Elsevier Ltd and Techna Group S.r.l. All rights reserved.
doi:10.1016/j.ceramint.2012.01.051

Instead of avoiding the MgO hydration, another alternative consists of using the magnesia as a hydraulic binder, where the brucite precipitation should be mastered in order to enhance the castables mechanical strength. The development of a magnesia based-binder would lead to a positive technological and economical impact in the refractory field due to its performance and lower cost, when compared to calcium aluminate cements. Recently, a novel binder based on dead-burnt magnesia particle size optimization was evaluated [14]. In addition, Sandberg and Mosberg [12] analyzed the bonding effect in the MgO–SiO_2 system pointing out that magnesia can react with water and silica fume, resulting in a castable material with suitable green mechanical strength.

Considering these aspects, this work addresses: (1) the role of three magnesia sources (dead-burnt or caustic ones) with distinct reactivity in CAC-containing castable compositions; and (2) the MgO and MgO–SiO_2 bonding effect attained for different magnesia sources in cement-free castables. Moreover, as new experimental methodologies are still required in order to allow a more accurate analysis of the damage caused by the MgO hydration process, the Young's modulus (E) measurements were used in this work during the refractory curing and drying steps. The collected results were compared and analyzed with those attained by the usual mechanical strength tests.

2. Experimental

A dead-burnt (DB) and two caustic magnesias (CM1 and CM2) (Magnesita Refratários S.A., Brazil) with specific surface areas of 1.1 m^2/g, 11.1 m^2/g and 24.6 m^2/g, respectively, were selected. Their physical properties and chemical compositions are presented in Table 1.

Vibratable alumina–magnesia castable compositions containing different silica fume (971 U, Elkem, Norway) and calcium aluminate cement (Secar 71, Kerneos, France) amounts were designed according to the Alfred's particle packing model ($q = 0.26$) [15]. Coarse tabular alumina was added as aggregates ($d \leq 6$ mm, Almatis, USA) and the matrix fraction comprised magnesia (DB, CM1 or CM2), reactive alumina (CL370, Almatis, USA) and fine ($\leq$200 μm) tabular alumina (Almatis, USA). Reference compositions without magnesia and containing 2, 4 or 6 wt% of calcium aluminate cement were also evaluated. The castable dispersion was carried out by adding a polycarboxylate based dispersant (Basf, Germany). General information regarding the compositions and the water content required for their appropriate mixing and moulding are presented in Tables 2 and 3, respectively.

Table 1
Physical properties and chemical compositions of the selected magnesia sources.

MgO source	DB	CM1	CM2
Physical and chemical properties			
SSA (m^2/g)	1.1	11.1	24.6
D_{10} (μm)	0.55	2.05	2.00
D_{50} (μm)	7.76	20.14	16.58
D_{90} (μm)	35.48	52.19	51.09
ρ (g cm^{-3})	3.53	3.20	3.38
Chemical composition (wt%)			
MgO	98.17	94.73	98.38
CaO	0.84	0.42	0.88
SiO_2	0.33	1.58	0.17
Al_2O_3	0.12	0.35	0.05
Fe_2O_3	0.41	2.06	0.42
MnO	0.13	0.86	0.10
CaO/SiO_2	2.54	0.27	5.18

SSA = specific surface area. D_{90}, D_{50} and D_{10} = equivalent spherical particles diameter (weight below 90, 50 and 10, respectively). ρ = density.

After mixing, the prepared samples were placed in a climatic chamber (Vöetsch 2020, Germany) at 50 °C in an environment with relative humidity close to 80%. The initial castable hydration process (curing step) was evaluated for 7 days using Young's modulus and mechanical strength measurements.

Prismatic samples (25 mm × 25 mm × 150 mm) were cast under vibration and carefully demoulded after 3 h of curing for the Young's modulus evaluation. These measurements were carried out according to ASTM C 1198-91 using the resonance bar technique (Scanelastic equipment, ATCP, Brazil), which is based on the sample excitation and by the detection of the correspondent vibration spectrum, using piezoelectric transducers. In such experiments, a wide frequency scanning is performed in order to excite and capture the natural resonance frequencies of the bars. The elastic modulus is calculated based on the resulted vibration spectrum applying Pickett equations, which correlates the elastic modulus, the natural vibration frequencies and the sample dimensions [16]. For the fundamental flexural frequency of a rectangular bar, the Young's modulus is given by:

$$E = 0.9465 \frac{m f_f^2}{b} \times \frac{L^3}{t^3} \times T_1 \quad (1)$$

where E is the Young's modulus (Pa), m the mass (g), b the width (mm), L the length (mm), t the thickness (mm), f_f the fundamental resonance frequency of the bar in flexure (Hz), and T_1 the correction factor for fundamental flexural mode to account for finite thickness of the bar, Poisson's ratio and others.

Cylindrical specimens (40 mm × 40 mm) were also cast and cured for the splitting tensile strength (ASTM C496-90) and thermogravimetric evaluations. The mechanical tests were conducted in MTS testing equipment (MTS Systems, Model 810, USA) using a constant loading rate of 42 N/s. The splitting tensile strength was calculated by:

$$\sigma_f = 2 \times \left(\frac{P}{\pi L D} \right) \quad (2)$$

where σ_f is the splitting tensile stress (MPa), P is the maximum load (N), L (mm) and D (mm) are the height and diameter of the samples, respectively.

Some drying tests were carried out up to 600 °C in green humid samples (cured at 50 °C for 24 h) and dried ones (110 °C for 24 h), under a 10 °C min^{-1} heating rate, using a thermogravimetric apparatus [17]. Mass changes and the

Table 2
Refractory castables compositions evaluated in this work.

Raw materials	Content (wt%)									
	Binder and MgO-containing castables			Binder-containing and MgO-free castables			Binder-free and MgO-containing castables			
	2C1S	4C1S	6C1S	2C1S	4C1S	6C1S	0C0S	0C1S	0C2S	0C4S
Tabular alumina ($d \leq 6$ mm)	80	80	80	80	80	80	81	80	79	77
Reactive alumina (CL370)	11	9	7	11	9	7	7	7	7	7
Fumed silica (971 U)	1	1	1	1	1	1	0	1	2	4
Magnesia (DB or CM1 or CM2)	6	6	6	0	0	0	6	6	6	6
Calcium aluminate cement (Secar 71)	2	4	6	2	4	6	0	0	0	0
Tabular alumina ($d < 45$ μm)	0	0	0	6	6	6	6	6	6	6
Dispersant	0.2	0.2	0.2	0.2	0.2	0.2	0.2	0.2	0.3	0.4

temperature profile of the furnace and of the samples' surface were simultaneously recorded. Percent mass loss rate (dW/dt, wt% min^{-1}) versus samples' temperature curve was used for the drying behavior evaluation [8,14].

3. Results and discussion

3.1. Elastic modulus technique as a tool for the magnesia hydration evaluation

According to the specific surface area values, the chosen DB, CM1 and CM2 magnesia sources can be classified as materials with low, medium-high and high reactivity, respectively. In order to analyze the potential of the Young's modulus technique as a tool for the magnesia hydration analysis, dead-burnt (DB) and a caustic magnesia source (CM2) were firstly added to two different castable compositions: (a) cement-free (0C1S) or (b) containing 6 wt% of calcium aluminate cement (6C1S), both with 1 wt% of silica fume (Table 2). Fig. 1 presents the measured elastic modulus and mechanical strength with the curing time for CM2 or DB-containing castables.

For the CM2-6C1S samples, the evaluated values increased at the initial curing stage, reaching their maximum at distinct curing days: close to the second for Young's modulus and the third for splitting tensile strength. Both samples containing caustic magnesia (CM2) presented elastic modulus decrease over time (Fig. 1a), which is associated with their expansion and the lack of ability to accommodate the brucite formation, leading to cracks generation [18]. Due to the lower reactivity of the dead-burnt magnesia, a continuous increase in the DB-6C1S and DB-0C1S mechanical strength and stiffness were observed along the curing period at 50 °C and no damage related to the $Mg(OH)_2$ formation was detected (Fig. 1b). For this MgO source, as new phases are generated (i.e., cement hydrates, brucite, etc.), new bonds between particles are formed, improving the castables' properties.

The CAC–water reaction involves the hydrate precipitation (mainly, CAH_{10}, C_2AH_8, C_3AH_6 and AH_3, where C = CaO, $A = Al_2O_3$ and $H = H_2O$) and crystal growth, which link the particles and change the samples' porosity over time. Therefore, the higher mechanical strength and elastic modulus of the cement bonded samples (CM2-6C1S and DB-6C1S) is related to the role of these hydrates. However, although this aspect should allow greater physical expansion without damage, the

Table 3
Water content added during the refractory castables mixing step.

Compositions	Water content (wt%)						
	2C1S	4C1S	6C1S	0C0S	0C1S	0C2S	0C4S
DB	4.0	4.1	4.2	4.0	4.1	4.1	4.2
CM1	4.8	5.0	5.3	5.1	5.2	5.2	5.4
CM2	5.1	5.5	5.9	5.1	5.8	6.1	6.4
MgO free	4.0	4.1	4.2	-	-	-	-

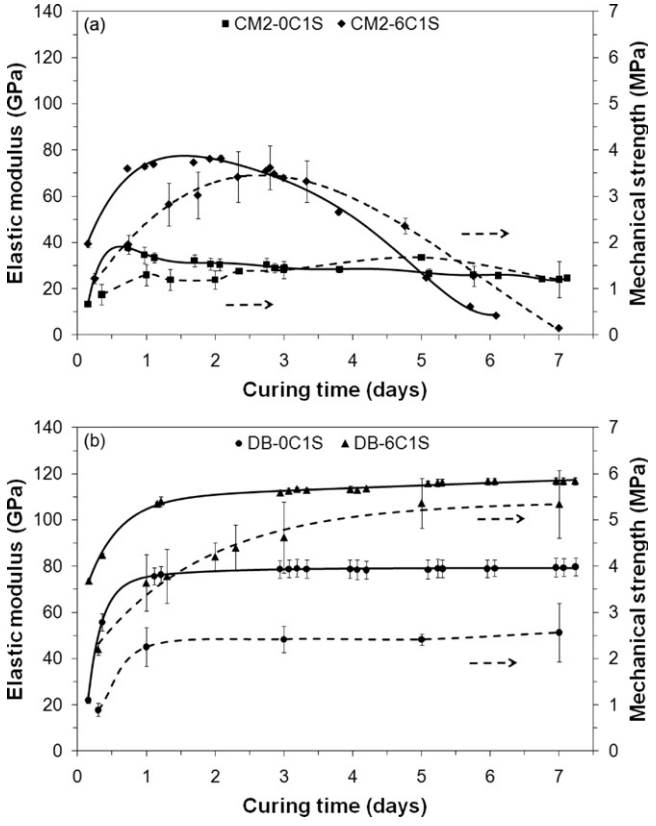

Fig. 1. Elastic modulus and mechanical strength as a function of curing time. Castables containing (a) CM2 or (b) DB magnesia, with (CM2-6C1S and DB-6C1S) or without cement (CM2-0C1S and DB-0C1S).

lower initial porosity of these castables can also reduce the likelihood of $Mg(OH)_2$ accommodation [6], spoiling their properties.

Considering the attained elastic modulus results, when compared to the mechanical strength ones, it can be concluded that the former technique presents some advantages related to accuracy, the fact of being a non-destructive test and allowing a suitable analysis of the castables curing evolution. Therefore, this first set of results highlights the importance of the Young's modulus measurements when evaluating the physical damage in the castables' structure (that cannot be visually identified) during the curing step.

3.2. Magnesia sources effect on the cement-bonded castables performance

The performance of three magnesia sources (DB, CM1, CM2) were evaluated in castable compositions containing 2, 4 or 6 wt% of calcium aluminate cement and 1 wt% of silica fume. Moreover, magnesia-free compositions (with 2, 4 or 6 wt% of cement and 1 wt% of silica fume) were designed and prepared to be used as reference materials.

Fig. 2 presents the thermogravimetric results (drying tests) for samples cured at 50 °C/24 h and dried at 110 °C/24 h. When increasing the cement content, higher drying rate peak areas are attained for the magnesia-free castables (Fig. 4a), which is related to the amount of hydrated phases of the samples. The presence of cement hydrates should be observed at temperatures lower than 400 °C, as the C_2AH_8, AH_3 and C_3AH_6 phases decompose in the temperature range of 180–360 °C [13]. Nevertheless, some displacements of the peak positions were detected due to the samples volume, porosity, permeability and furnace heating rate (~10 °C min^{-1}).

The $Mg(OH)_2$ decomposition was detected above 350 °C for the MgO-containing castables (Fig. 2b–d) and the magnesia reactivity associated with the presence of CAC and silica fume clearly affected the formation of such hydroxide. According to some authors [19], during the cement hydration, calcium aluminates dissolution will lead to a significant increase in the suspension pH. Consequently, due to the chemical equilibrium shifting principle, dead-burnt magnesia hydration is favored, whereas the reaction of the caustic one should not be influenced by this parameter, as the latter presents higher reactivity and its hydration causes a major increase in the castable pH values [10]. In addition, although silica fume should not be hydrated [20], when in contact with basic suspensions as these ones, its dissolution can induce the formation of an insoluble magnesium silicate coating at magnesia's particles surface, reducing the hydration rate [7]. Both factors (CAC and SiO_2 effects) must be considered when evaluating the thermogravimetric results (Fig. 2).

For the DB-containing compositions (Fig. 2b), the combined presence of CAC and silica fume hindered the hydration process and the $Mg(OH)_2$ decomposition peak was not observed for the cement containing compositions. It is believed that CAC hydration favored the silica fume dissolution, improving the efficiency of this oxide to act as an anti-hydration additive. However, additional adjustments in the SiO_2 content should be carried out in order to control the hydration of magnesia sources with higher specific surface area, as the caustic sources.

Regarding the caustic magnesias, the drying rate peak area of the brucite phase increases when reducing the CAC content

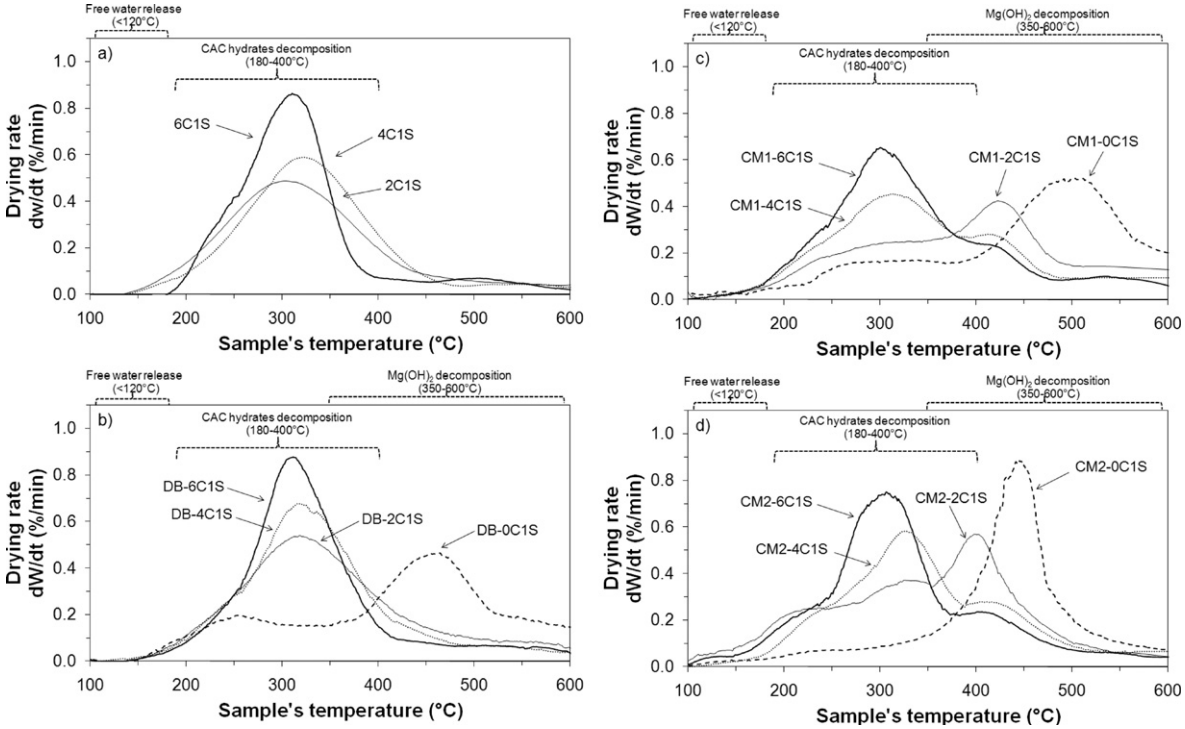

Fig. 2. Drying rate profiles as a function of sample's temperature for castables with different cement contents (6C1S, 4C1S, 2C1S or 0C1S) after curing at 50 °C/24 h and drying at 110 °C/24 h: (a) MgO-free, or containing (b) DB, (c) CM1, and (d) CM2.

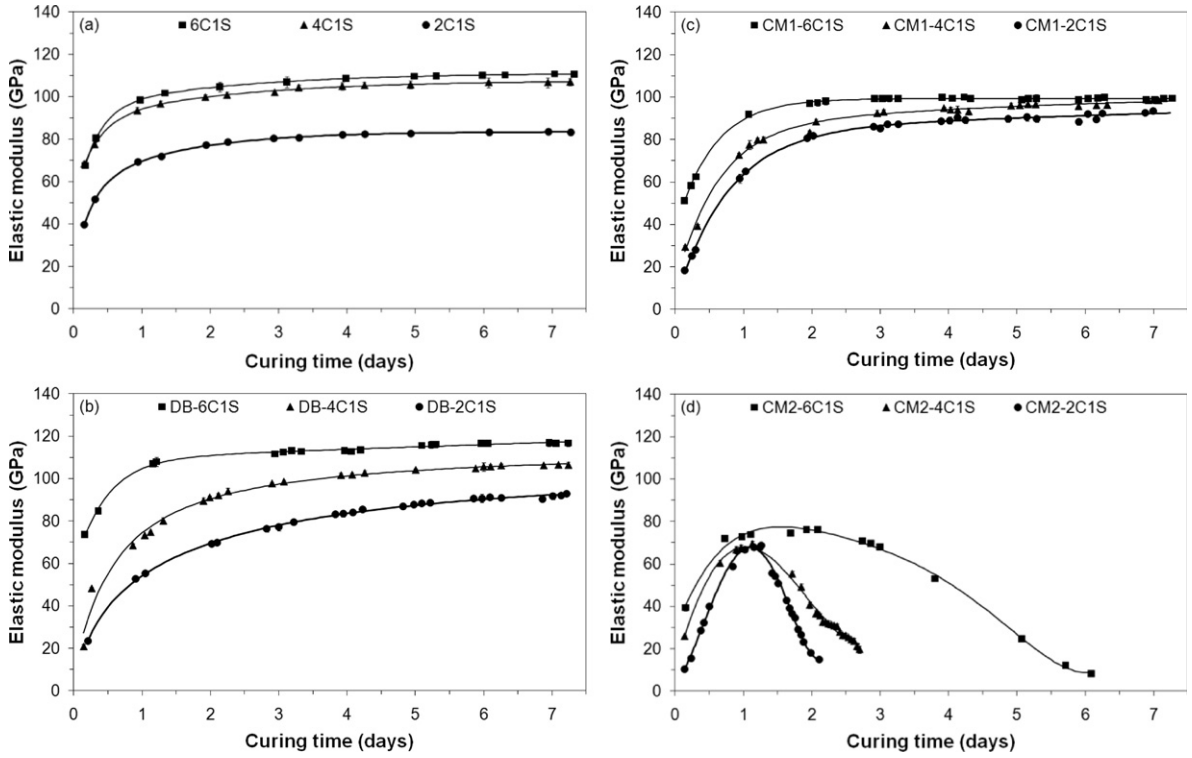

Fig. 3. Elastic modulus as a function of curing time for castables with different cement contents (6C1S, 4C1S or 2C1S): (a) MgO-free, or containing (b) DB, (c) CM1, and (d) containing CM2.

added to CM1 and CM2 compositions (Fig. 2c and d). Hence, due to the competition between magnesia and cement to consume water during the castable preparation, higher liquid amount would be available to react with magnesia when decreasing the cement content. The higher reactivity of these magnesia sources also played a role in the attained results, speeding up the negative effects caused by the expansive behavior of $Mg(OH)_2$ (as presented in Fig. 3).

As mentioned in the previous (Section 3.1), 6 wt% of cement resulted in samples with the highest elastic modulus values throughout the 7 days of curing at 50 °C for the evaluated materials. Few changes between the MgO free samples and the DB-containing compositions behavior were observed in Fig. 3a and b (E values were in the range of 20–110 GPa) due to the absence of $Mg(OH)_2$ formation in both group of materials. Conversely, the change of the CAC content from 6 to 2 wt% in the CM1 samples (Fig. 3c) was followed by higher brucite formation (Fig. 2c) and the expected stiffness decay did not take place due to the bonding effect of this hydroxide phase and packing pore closure. These samples also presented elastic modulus values close to the ones of the reference materials (E = 100 GPa) on the 7th day of curing. Therefore, regardless of its reactivity, this caustic magnesia source (CM1) can be applied in refractory compositions when in the presence of anti-damage and anti-hydration additives (cement and silica fume, respectively).

On the other hand, higher amounts of brucite were detected when CM2 magnesia were added to the castable compositions (Fig. 2d), inducing a great reduction in the samples elastic modulus due to the crack nucleation and propagation (Fig. 3d). According to these results, the MgO source reactivity should be considered for the selection of the calcium aluminate cement content in order to delay or inhibit the drawbacks caused by the $Mg(OH)_2$ phase.

3.3. Magnesia hydration bonding effect on cement-free compositions

Considering the MgO or MgO–SiO_2 bonding effect, some castable compositions comprising DB, CM1 or CM2 magnesia sources and distinct silica fume contents (1, 2 or 4 wt%) were evaluated by thermogravimetric and elastic modulus techniques. Fig. 4 presents the elastic modulus evolution with the curing time. For the silica free compositions (Fig. 4a), the E values increase was observed at an early age (between 0 and 12 h), attesting that the magnesia bonding effect is induced when the formed magnesium hydroxide phase can be accommodated in the castable structure.

For longer curing times, CM1-0C0S samples showed a continuous stiffness increase up to the seventh day and the magnesia hydration also led to a positive effect on their performance. Conversely, the elastic modulus decay of the CM2-0C0S and DB-0C0S was observed after 12 h and 3 days, respectively, as the tensile stresses generated by the brucite formation exceeded the mechanical strength and resulted in the materials cracking.

Besides the amount of $Mg(OH)_2$ generated in the hydrated samples, the water content for the samples preparation (Table 3) should also affect their porosity and other properties [21]. Although the porosity in the castable samples can better accommodate the in situ formed brucite crystals, their lower

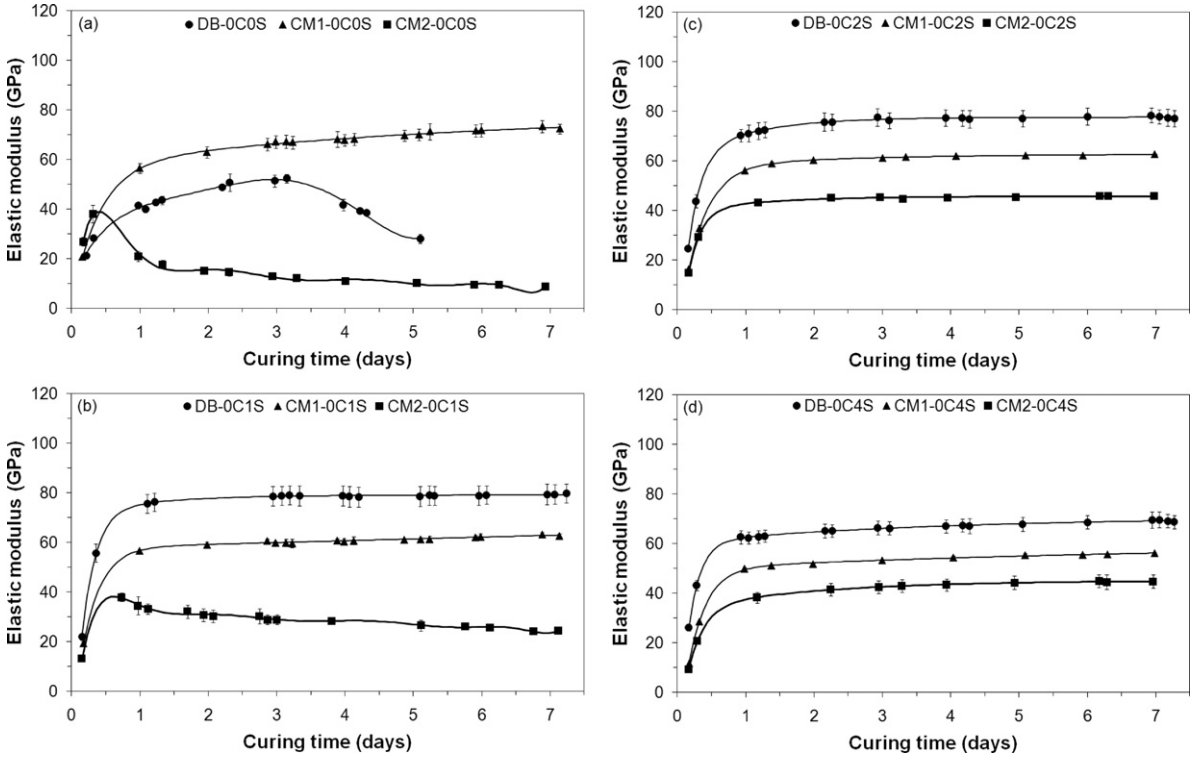

Fig. 4. Elastic modulus as a function of curing time for castables with different MgO sources (DB, CM1 or CM2) and silica fume contents: (a) 0 wt% (0C0S), (b) 1 wt% (0C1S), (c) 2 wt% (0C2S), and (d) 4 wt% (0C4S).

mechanical resistance will withstand lower levels of tensile strain due to expansion.

During the magnesite ($MgCO_3$) heat treatment for the production of dead-burnt MgO, the impurities do not remain as free oxides, but combine or react with magnesia (such as, films at the grain boundaries or incorporated into solid solution) improving the hydration resistance of the final product [22]. The CaO/SiO_2 ratio of the system will define which secondary phases can be generated in the dead-burnt magnesia composition. For high CaO/SiO_2 values, there is a greater likelihood of finding free CaO in those materials and this oxide can readily react with water and induces higher volumetric expansion during the castables curing and drying steps. In addition, the calcining temperature of the CM1 and CM2 magnesias is close to 1000 °C, which does not allow a further reaction between CaO and SiO_2 to form $2CaO{\cdot}SiO_2$ and/or $3CaO{\cdot}SiO_2$ phases [22]. Therefore, the presence of free CaO and SiO_2 in those caustic magnesias affected the elastic modulus evolution of the CM1 and CM2 containing compositions (Fig. 4a). According to the information provided by the raw materials supplier, after the thermal treatment at 1000 °C, fine silica particles could be found between the crystalline MgO grains and this secondary phase should act in a similar manner as the silica fume additive, reducing the hydration [7]. Due to its lower free CaO content (0.42 wt%) and higher SiO_2 amount (1.58 wt%), when compared to CM2 magnesia source (Table 1), the CM1-0C0S containing castable was the only composition that did not present crack formation during the curing step (Fig. 4a).

Nevertheless, the addition of 1 wt% of silica fume led to important changes of the elastic modulus values (Fig. 4b). The lubricant effect of this additive (due to its spherical morphology and small particle size) favors the particles packing, filling in the available interstices and, consequently, reducing the porosity of the castables [23]. Thus, DB-0C1S displayed an increase in the elastic modulus values and no cracks formation. CM2-0C1S results kept the elastic modulus decreasing profile, but a delay of the stiffness decay was observed due to the silica anti-hydration action (Fig. 4b). Conversely, the limited magnesium hydroxide formation in the CM1-0C1S samples resulted in the decrease of the E values when compared to the SiO_2 free materials (Fig. 4a and b).

Based on the additional thermogravimetric tests conducted for the CM2 samples, one could conclude that the use of 1, 2 or 4 wt% of SiO_2 decreased the amount of the formed $Mg(OH)_2$,

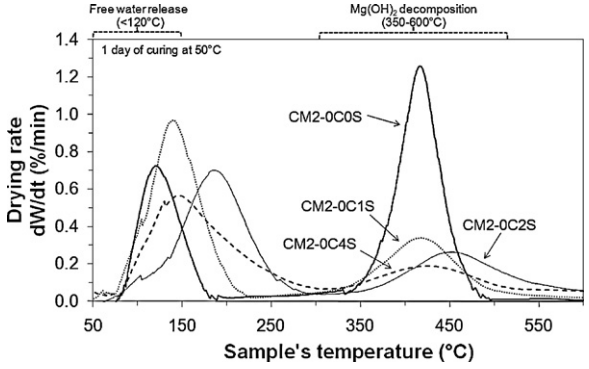

Fig. 5. Drying rate profiles as a function of sample's temperature after 1 day of curing at 50 °C for CM2-containing castables with different silica fume contents: 0 wt% (0C0S), 1 wt% (0C1S), 2 wt% (0C2S), and 4 wt% (0C4S).

as the area of the peaks located between 350 °C and 600 °C is proportional to the decomposition of this hydroxide compound (Fig. 5).

Moreover, according to the elastic modulus behavior presented in Fig. 4c and d, the addition of 2 and 4 wt% did not lead to major changes in the DB and CM1 containing samples properties, whereas no damage was detected for the CM2 compositions in the evaluated curing time.

A suitable analysis of the attained Young's modulus results must take into account: (1) the amount of brucite formation; (2) the changes in the tabular alumina aggregates content due to the silica fume addition; and (3) the water content used in the castables processing step. Therefore, based on the silica free compositions results (Fig. 4a), when the crack formation does not take place (CM1-0C0S), higher $Mg(OH)_2$ contents should lead to greater elastic modulus values. On the other hand, the decrease in the E value is expected to occur by reducing the alumina aggregates, as the stiffness of the α-Al_2O_3 crystals is close to 390 GPa, whereas fused silica and quartz ones are 70 and 95 GPa, respectively [24,25]. Furthermore, SiO_2 hinders the brucite formation and consequent pore closure, inducing the decrease of Young's modulus.

In general, silica fume additions require an increase in the water content for a suitable sample casting (Table 3). However, higher water amount does not affect significantly the magnesia hydration degree [26], but spoils the castables mechanical strength and elastic modulus, as these properties are directly correlated. Another drawback caused by the SiO_2 addition is related to the samples permeability decrease, inducing a delay in their drying process [27].

Despite these aspects, SiO_2 is considered an efficient additive to control MgO hydration. As presented in Fig. 4, the addition of 1, 2 and 4 wt% of silica fume to the DB and CM2-containig castables reduced the magnesia hydration, inhibited crack formation and the elastic modulus decrease.

4. Conclusions

Different features can be highlighted based on the attained results, which can be summarized as follows:

- The measurements of Young's modulus using the resonance bar technique is a suitable and efficient procedure to evaluate the MgO hydration damage generated in the refractory castables structure during the curing and drying step. By using this non-destructive method, the crack formation was detected earlier when compared with mechanical tests, which reinforces its higher accuracy when analyzing the castables' microstructural evolution over time.
- The use of optimized calcium aluminate cement amounts in castables containing caustic magnesia sources (CM1 and CM2) is required in order to inhibit the damage derived from the higher water reactivity of these materials. The addition of 6 wt% of cement provided a suitable condition to avoid crack formation and the elastic modulus decrease for the DB and CM1 compositions. Nevertheless, the use of higher cement contents or anti-hydration additives should be considered for the production and properties of refractory castables containing CM2 magnesia.
- Under certain conditions, MgO can be applied as a binder (replacing calcium aluminate cement), leading to a significant reduction in the castables' costs without the drawback of forming low melting temperature phases as observed in the CAC containing system. The designed cement-free castables' compositions, which present high alumina content, are located within the alumina-mullite-spinel compatibility triangle of the Al_2O_3–MgO–SiO_2 phase diagram, where the formation of liquid phases is expected to take place above 1578 °C in a thermodynamic equilibrium condition.
- All tested magnesia sources (DB, CM1 and CM2) have the potential to be used as a binder, but the low CaO/SiO_2 ratio is one of the main requirements for controlling the bonding effect and the physical integrity of the castable samples.
- Al_2O_3–MgO cement-free compositions containing silica fume as an anti-hydration additive can be a suitable alternative to induce better particle packing, resulting in the increase of the castable mechanical strength after curing.

Acknowledgments

The authors are grateful to the Magnesita Refratários S.A. (Brazil), FIRE and CNPq for supporting this work.

References

[1] M.A.L. Braulio, D.H. Milanez, E.Y. Sako, L.R.M. Bittencourt, V.C. Pandolfelli, Are refractory aggregates inert? Am. Ceram. Soc. Bull. 87 (3) (2007) 27–32.
[2] M.A.L. Braulio, L.R.M. Bittencourt, J. Poirier, V.C. Pandolfelli, Microsilica effects on cement bonded alumina–magnesia refractory castables, J. Tech. Assoc. Refract. Jpn. 28 (3) (2008) 180–184.
[3] M.A.L. Braulio, L.R.M. Bittencourt, V.C. Pandolfelli, Magnesia grain size effect on in situ spinel refractory castables, J. Eur. Ceram. Soc. 28 (2008) 2845–2852.
[4] H.S. Tripathi, B. Mukherjee, S. Das, M.K. Haldar, S.K. Das, A. Ghosh, Synthesis and densification of magnesium aluminate spinel: effect of MgO reactivity, Ceram. Int. 29 (2003) 915–918.
[5] M.A.L. Braulio, J.F.R. Castro, C. Pagliosa, L.R.M. Bittencourt, V.C. Pandolfelli, From macro to nano magnesia: designing the in situ spinel expansion, J. Am. Ceram. Soc. 91 (9) (2008) 3090–3093.
[6] R. Salomão, L.R.M. Bittencourt, V.C. Pandolfelli, A novel approach for magnesia hydration assessment in refractory castables, Ceram. Int. 33 (2007) 803–810.
[7] R. Salomão, V.C. Pandolfelli, Microsilica addition as anti-hydration technique of magnesia in refractory castables, Cerâmica 54 (2008) 43–48 (in Portuguese).
[8] R. Salomão, V.C. Pandolfelli, The role of hydraulic binders on magnesia containing refractory castables: calcium aluminate cement and hydratable alumina, Ceram. Int. 35 (2009) 3117–3124.
[9] A. Yoschida, T. Nemoto, A. Kaneyasu, Evaluation method for hydration resistance of magnesia fine power and effect of B_2O_3 content in magnesia raw materials, in: Proc. Unified Int. Tech. Conf. Refractories UNITECR'03, Osaka, Japan, (2003), pp. 433–436.
[10] R. Salomão, L.F. Amaral, V.C. Pandolfelli, Effects of calcium aluminate cement addition on magnesia hydration, Cerâmica 56 (2010) 135–140 (in Portuguese).
[11] M.A.L. Braulio, D.H. Milanez, E.Y. Sako, L.R.M. Bittencourt, V.C. Pandolfelli, Expansion behaviour of cement-bonded alumina–magnesia refractory castables, Am. Ceram. Soc. Bull. 86 (12) (2007) 9201–9206.

[12] B. Sandberg, T. Mosberg, Use of microsilica in binder systems for ultra-low cement castables and basic, cement-free castables, Ceram. Trans. 4 (1989) 245–258.
[13] W.E. Lee, W. Vieira, S. Zhang, K. Ghanbari Ahari, H. Sarpoolaky, C. Parr, Castable refractory concretes, Int. Mater. Rev. 46 (3) (2001) 145–167.
[14] R. Salomão, L.R.M. Bittencourt, V.C. Pandolfelli, A novel magnesia based binder (MBB) for refractory castables, Interceramic 58 (2009) 21–24.
[15] R.G. Pileggi, A.R. Studart, M.D.M. Innocentini, V.C. Pandolfelli, High performance refractory castables, Am. Ceram. Soc. Bull. 81 (2002) 37–42.
[16] G. Pickett, Equations for computing elastic constants from flexural and torsional resonant frequencies of vibration of prisms and cylinders, Proc. Am. Soc. Testing Mater. 45 (1945) 846–865.
[17] M.D.M. Innocentini, F.A. Cardoso, M.M. Akyioshi, V.C. Pandolfelli, Drying stages during the heating of high-alumina, ultra-low-cement refractory castables, J. Am. Ceram. Soc. 86 (7) (2003) 1146–1148.
[18] P. Lauzon, J. Rigby, C. Oprea, T. Troczynski, G. Oprea, Hydration studies on magnesia-containing refractories, in: Proc. Unified Int. Tech. Conf. Refractories, UNITECR'03, Osaka, Japan, (2003), pp. 54–57.
[19] J.R. Garcia, I.R. de Oliveira, V.C. Pandolfelli, Hydration process and the mechanisms of retarding and accelerating the setting time of calcium aluminate cement, Cerâmica 53 (2007) 42–56 (in Portuguese).
[20] K.G. Ahari, J.H. Sharp, W.E. Lee, Hydration of refractory oxides in castable bond systems II: alumina–silica and magnesia–silica mixtures, J. Eur. Ceram. Soc. 22 (2002) 495–503.
[21] F.T. Ramal Jr., R. Salomão, V.C. Pandolfelli, Water content and its effect on the drying behaviour of refractory castables, Ref. Appl. News 10 (3) (2005) 10–13.
[22] R.A. Landy, Magnesia Refractories, in: C.A. Schacht (Ed.), Refractories Handbook, Marcel Dekker Inc., New York, 2004, pp. 109–149.
[23] B. Myrhe, B. Sandberg, The Use of Microsilica in Refractory Castables. Available in: www.refractories.elkem.com/dav/b360ef3589.PDF (accessed on January 2012).
[24] R.G. Munro, Evaluated material properties for a sintered α-alumina, J. Am. Ceram. Soc. 80 (8) (1997) 1919–1928.
[25] W.C. Oliver, G.M. Pharr, An improved technique for determining hardness and elastic modulus using load and displacement sensing indentation experiments, J. Mater. Res. 7 (6) (1992) 1564–1583.
[26] R. Salomão, V.C. Pandolfelli, Reducing the damages of MgO hydration on refractory castables, in: Proc. Unified Int. Tech. Conf. Refractories UNITECR'09, Salvador, Brazil, (2009), p. 56.
[27] R.D. dos Anjos, M.R. Ismael, F.T. Ramal Jr., V.C. Pandolfelli, Microsilica addition and the drying of refractory castables, Cerâmica 50 (2004) 331–335 (in Portuguese).